# PROBLEM NO. FAC-4

**Title: Predicting Ductile Tearing and Residual Strength of a Flat Sheet with/without MSD Objective:**

To illustrate the process of using the nonlinear finite element method to predict stable, ductile tearing and to evaluate the residual strength of a flat sheet containing multi-site damage.**General Description:**

This problem details the process of using the finite element method to predict the residual strength of a simple flat plate containing a single crack, or a lead crack with MSD. A criterion for stable, ductile tearing based on the crack tip opening angle ($CTOA_c$) is introduced. Bases for this criterion are discussed, and experimental and computational investigations of it are described and evaluated for guidelines in use. Example simulations are then detailed. These include one of an MT specimen containing a single crack, and five involving various configurations of MSD. Predictions of crack growth and linkup, of residual strength, and of effect of MSD on decrease in residual strength are presented.

*Topics Covered*: Finite element analysis, stable tearing, MSD, residual strength, non-linear fracture mechanics

*Type of Structure*: flat sheet with single crack or cracks with MSD

**Relevant Sections of Handbook:** Sections 2, 3, 4, 5, 11

**Author:** Dr. A. R. Ingraffea

**Company Name**: Fracture Analysis Consultants, Inc.

121 Eastern Heights Drive
Ithaca, NY 14850
607-257-4970
www.fracanalysis.com

**Contact Point:** Dr. Paul Wawrzynek
**Phone:** 607-257-4970
**e-Mail:** wash@fracanalysis.com

Fracture Analysis
Consultants, Inc.

## Overview of Problem Description

An important element in the process of predicting residual strength of a structure experiencing ductile tearing is having a criterion that predicts the onset and rate of this phenomenon. Tests and numerical simulations have been performed to assess the critical crack tip opening angle ($CTOA_c$) criterion for predicting residual strength of structures containing MSD. The objectives of this problem are to describe the bases for this criterion and to present example simulations that employ it. The next section details the theoretical background behind the $CTOA_c$ criterion, and describes experimental and computational investigations into it. This section is followed by a review of findings of these investigations. Those readers wanting to go directly to a computational example application of this criterion can proceed directly to the **Computational Models** section.

The *$CTOA_c$ Criterion for Ductile Tearing*

The local slope of the crack tip opening profile, or CTOA, has been suggested to characterize ductile crack growth behavior [de Koning 1977]. Newman [1984], Rice and Sorensen [1978], and Kanninen and Popelar [1985] further defined the CTOA as the crack tip opening angle measured at a fixed distance behind the moving crack tip. The CTOA fracture criterion asserts that this angle maintains a constant value during stable crack growth for a given thickness of material.

The definition of CTOA as suggested by Newman [1984] is adopted for this problem. For Mode-I only deformations, CTOA is defined as, Figure FAC-4.1:

$$CTOA = 2\,tan^{-1}\frac{\delta}{2d}$$

where *d* is the CTOD measured at a specific distance, d, behind the crack tip.

Stable crack growth is an inherent feature of elastic-plastic materials because of the occurrence of permanent plastic deformations during unloading [Rice 1975]. This effect can be demonstrated by global energy dissipation or by the local residual plastic deformations. Suppose two materials have the same uniaxial stress-strain curves; one is an idealized nonlinear elastic material and the other is an elastic-plastic material. For cases without crack growth, the same CTOA and strain concentration will occur in the two materials as illustrated in Figure FAC-4.2, STAGE 0. As the crack propagates in the nonlinear elastic material, deformation fields need to be readjusted and the same crack tip opening profile would occur for the new crack tip location. This is not the case for the elastic-plastic material because a large part of the energy is consumed by plastic dissipation with far less strain recovered during unloading. Thus, a smaller CTOA is obtained after crack growth (STAGE 1). Further increase of the applied loading is needed to open the crack (STAGE 2) and causes stable crack growth in the elastic-plastic material. Fracture instability will occur as the crack reaches a steady-state condition in which the crack continually advances without further increase in load. If the analysis is performed under displacement control, then a reduction in applied load is required to

maintain a constant CTOA for continuous crack growth. Hereafter, $CTOA_a$ is the crack tip opening angle measured immediately after propagation, STAGE 1. $CTOA_b$ is denoted as the increase in crack tip opening angle required to reach the critical value, $CTOA_c$. Thus, the condition

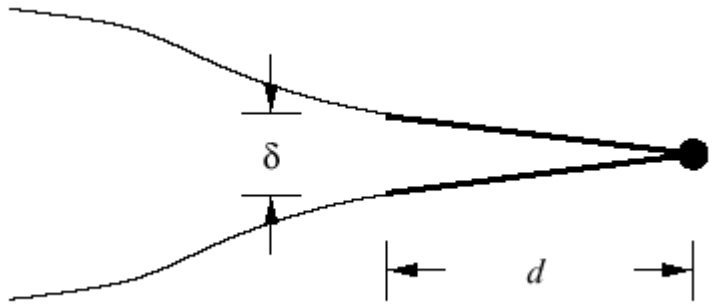


*Figure FAC-4.1. Illustration of parameters used for CTOA definition.*

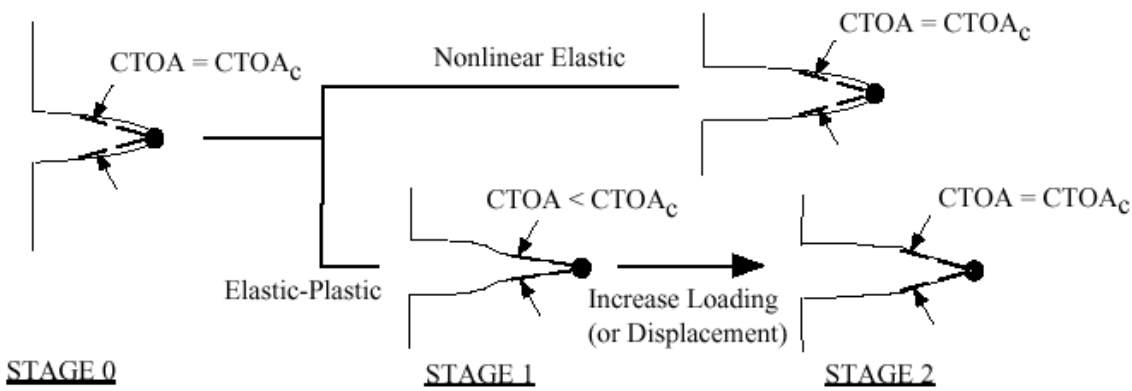


*Figure FAC-4.2. Illustration of crack growth in nonlinear elastic and elastic-plastic materials.*

$$CTOA_a + CTOA_b = CTOA_c$$

satisfies the fracture criterion for crack propagation, and the condition

$$CTOA_a = CTOA_c$$

indicates the occurrence of fracture instability for the analysis under load control. Another related factor for stable crack growth is the plastic wake effect caused by the residual plastic deformations [Newman 1984]. As the crack grows, the plastic zone behind the crack tip unloads to an elastic state leaving the appropriate plastic wake behind the advancing crack tip. This effect results in resistance to crack tip opening as

illustrated in Figure FAC-4.3. The dashed curves in the plastic wake region show what the crack opening profile would have been if residual plastic deformations had not been retained in the material behind the advancing crack tip. This phenomenon is also essential for simulating the initiation of stable crack growth associated with high fatigue stress prior to tearing [Dawicke 1994b].

Laboratory tests have been conducted on flat panels made of aluminum alloys to measure $CTOA_c$ values [Dawicke 1994a; Newman 1993]. Numerical simulations using these values have been conducted using two-dimensional [Newman, 1992, 1993; Dawicke 1994b, 1995, 1997a], thin-shell [Chen 1996, 1997, 1998], and three-dimensional [Dawicke 1996, 1998, 1997b] finite element elastic-plastic crack growth analyses. These activities are first reviewed to highlight important findings. The latest results are then used as a starting point for the example simulations.

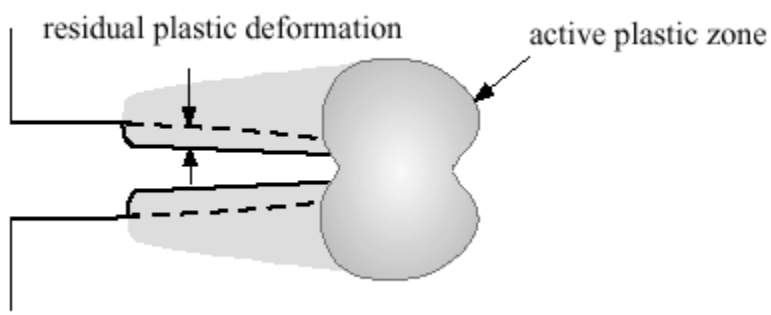


*Figure FAC-4.3. Illustration of plastic wake effect caused by crack growth.*

*Review of Findings on $CTOA_c$ Criterion*

A series of fracture tests has been conducted using a 2024-T3 aluminum alloy for MT, CT, blunt notch, THCT and MSD specimens. Newman *et al.* [1992] conducted tests on 0.05, 0.07, and 0.09 inch thick, 3.0 and 11.8 inch wide MT and blunt notch specimens as well as 0.09 inch thick, 10 inch wide THCT specimens. The blunt-notch specimen is similar to the MT specimen except that a small hole is drilled at both ends of the saw cut. It is intended to assess the suitability of elastic- plastic finite element analyses with the small-strain assumption to model large-scale plastic deformations. Good agreement between predicted and measured load versus notch-tip displacements substantiates the assumption. The critical values of CTOA were measured for the MT and THCT specimens to assert the specimen configuration independence of the fracture criterion. The THCT specimen had a stress intensity factor solution like that of a cracked, stiffened panel [Newman, 1995]. The measured $CTOA_c$ values showed higher angles at crack initiation, but reached the same constant value after a small transition period of crack growth. The agreement of $CTOA_c$ between MT and THCT specimens indicated that the $CTOA_c$ fracture criterion is independent of specimen configuration; this was further confirmed by a follow-up study with measurements from CT specimens [Dawicke 1995].

A 2D elastic-plastic finite element code, ZIP2D [Newman1974], and a 6.1 degree $CTOA_c$, computed at 0.01875 inch behind the crack tip, were used to simulate fracture behavior of the MT specimens [Newman 1992]. To model fatigue pre-cracking, cyclic loading simulation was conducted prior to stable tearing analyses. Experimental and predicted results showed that a higher applied stress during the fatigue tests increased the resistance to stable crack growth initiation. Predicted residual strengths under plane stress conditions were within 4% of experimental results for 3.0 and 11.8 inch wide MT specimens. However, the plane stress analyses over-predicted crack extension prior to limit load while the plane strain analyses under-predicted crack extensions.

The above studies raised two important questions:

1. What is the governing mechanism that causes higher $CTOA_c$ values during crack initiation?
2. What is the governing mechanism that causes the discrepancy between 2D predictions and test results?

Dawicke and Sutton [Dawicke 1994b] examined the higher values of measured $CTOA_c$ observed during crack initiation, i.e., question 1. Two independent techniques, optical microscopy (OM) and digital image correlation (DIC) were used to measure surface $CTOA_c$ during crack growth. The results of the two methods agreed very well. Fatigue marker loads and a scanning electron microscope were used to examine the fracture morphology and sequences of crack front profiles. For specimens under low magnitude of fatigue stress prior to tearing, crack surfaces underwent a transition from flat-to-slant crack growth. A schematic of the transition is shown in Figure FAC-4.4. During the transition period, the $CTOA_c$ values were high and significant tunneling occurred. After an amount of crack growth equal to about the specimen thickness, $CTOA_c$ reached a constant value. After crack growth equal to about twice the thickness, crack tunneling stabilized. For specimens that were pre-cracked under a high magnitude of fatigue stress, a 45-degree, slant, through-thickness initial crack was formed prior to tearing. During the crack initiation period, the $CTOA_c$ values of specimens with high fatigue stress were lower than the ones with low fatigue stress. But the same constant $CTOA_c$ value was observed after crack growth equal to about the specimen thickness.

The discrepancy between 2D predictions and test results, i.e., question 2, was thought to be related to the 3D constraint effect. Although thin-sheet structures behave essentially in plane stress, the constraint due to the finite thickness of the specimens can cause the regions local to the crack tip to approach plane strain conditions [Hom 1990]. To investigate the constraint effect, 2D and 3D analyses were conducted. In the 2D analyses, a core of elements above and below the crack path were assigned as plane strain while all other elements were assigned as plane stress. The plane strain core concept is illustrated in Figure FAC-4.5.

In their first attempt, Dawicke *et al.* [Dawicke 1995; Newman 1993] used 2D finite element analyses with a 6.0 degree $CTOA_c$ computed at 0.02 inch behind the crack tip and a plane strain core height equal to 0.2 inch to simulate fracture behavior with the constraint effect. They showed that the use of a plane strain core was essential to

accurately model crack growth. The predicted residual strengths were within 2% for 3 and 12 inch wide, 0.09 inch thick MT specimens and within 4% for 6 inch wide, 0.09 inch CT specimens. For 20 inch wide, 0.04 inch thick MSD specimens, 2D analyses with a 5.1 degree $CTOA_c$ showed excellent agreement of link-up and residual strength between predictions [Newman 1993] and test results [Broek 1994].

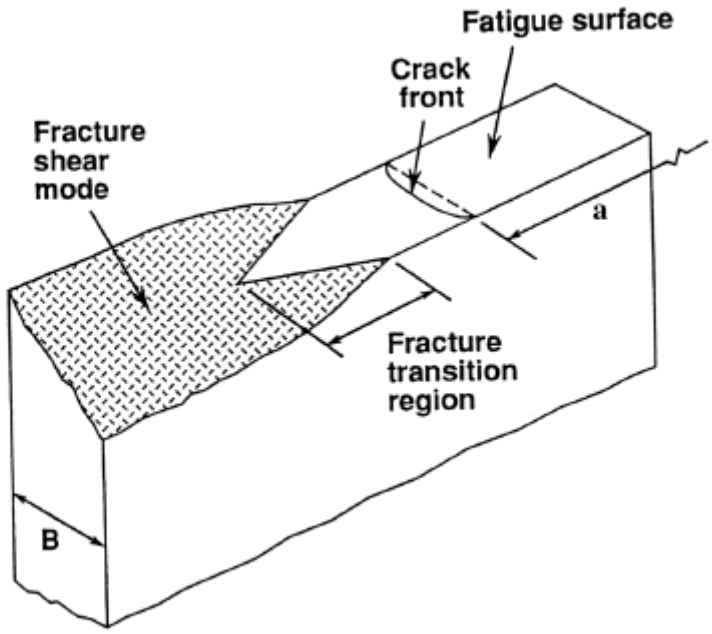


*Figure FAC-4.4. Schematic of fracture surface indicating transition from a flat to a slant crack plane (after [Newman 1992]).*

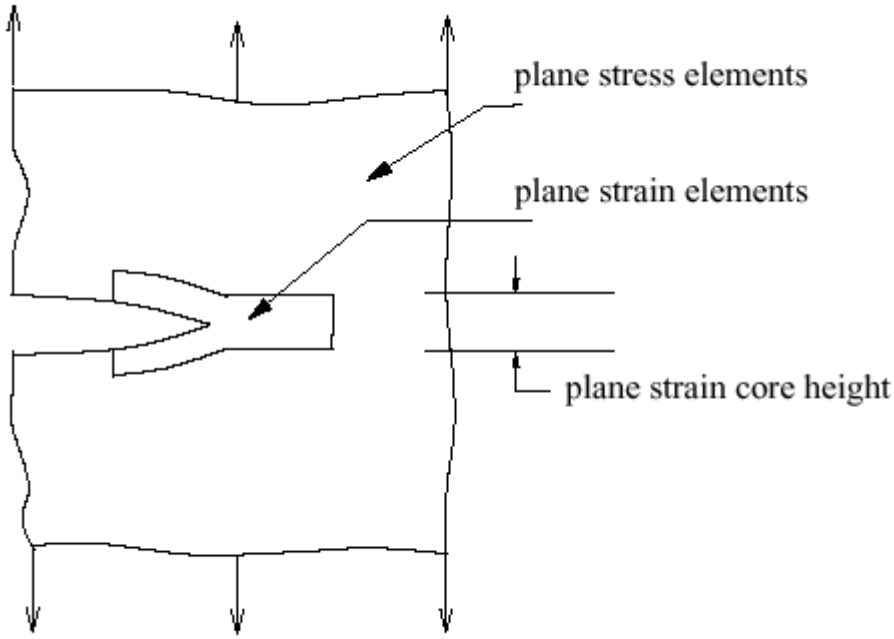


*Figure FAC-4.5. Schematic of the plane strain core.*

Dawicke et al. [Dawicke1996, 1998] further studied the constraint effect using 3D finite element analyses with a 5.25 degree $CTOA_c$ computed at 0.04 inch behind the crack tip. The 3D analyses successfully simulated fracture behavior of 2.0, 4.0, 6.0, and 8.0 inch wide CT specimens, 1.2, 3.0, 6.0, 12.0, 24.0, and 60.0 inch wide MT specimens, and 12.0 inch wide MSD specimens made of 0.09 inch thick, 2024-T3 aluminum alloy. A plane strain core height of 0.12 inch was required for 2D analyses to match the measured results and the 3D fracture predictions.

## Computational Models

In the following examples, tests on MT and MSD specimens are simulated. The FRANC3D/STAGS system [www.cfg.cornell.edu] is used to simulate fracture behavior and to predict residual strength using the guidelines derived from the 2D and 3D studies just described.

Fracture tests of MT specimens were conducted by the Mechanics of Materials Branch at NASA Langley Research Center [Dawicke 1994a, 1996,1998]. The test specimens were made of 0.09-inch thick 2024-T3 aluminum alloy. All specimens were fatigue pre-cracked in the L-T orientation with a low stress level that results in a stress intensity factor range of $\Delta K = 7$ ksi $\sqrt{\text{inch}}$. For specimens with a single crack, different widths of panels equal to 3 inch, 12 inch, and 24 inch with a crack-length to width ratio equal to 1/3 were tested, Figure FAC-4.6. For cases with multiple cracks, only the 12-inch wide specimens with two to five near collinear cracks as illustrated in Figure FAC-4.7 were tested. All tests were conducted under displacement control with guide plates to prevent

out-of-plane buckling. Both OM and DIC techniques were used to measure the $CTOA_c$ during stable crack growth [Dawicke 1994]. Experimental results for MT and CT specimens are shown in Figure FAC-4.8. The $CTOA_c$ rapidly reaches a constant value with a scatter band about ± 1 degree.

*Numerical Simulations of MT Specimens*

Fracture processes in the MT specimens are simulated first. To investigate panel size effects, numerical simulations of 60-inch wide panels with the same crack-length-to-width ratio are also performed. Elastic-plastic finite element analyses based on incremental flow theory with the von Mises yield criterion and the small strain assumptions are used to capture the active plastic zone and the plastic wake during stable crack propagation. A piecewise linear representation is used for the uniaxial stress-strain curve for 2024-T3 aluminum, Figure FAC-4.9. The $CTOA_c$ used in this study was 5.25 degrees measured 0.04 inch behind the crack tip. This particular value was provided by Dawicke and Newman [Dawicke 1996, 1998] based on 3D simulations of CT specimens. Upon satisfaction of the fracture criterion, nodal release and load (or displacement) relaxation techniques are employed to propagate the crack. Because of the double symmetry of the geometry and loading, only one-quarter of the specimen with imposed symmetry boundary conditions is modeled. Out-of-plane displacements are suppressed. Displacement-based, four-noded and five-noded quadrilateral shell elements having $C_1$ continuity are used [Rankin 1991]. These elements are intended to model thin shell structures for which transverse shear deformation is not important. Each node of the element has six degrees of freedom including three translations and three rotations.

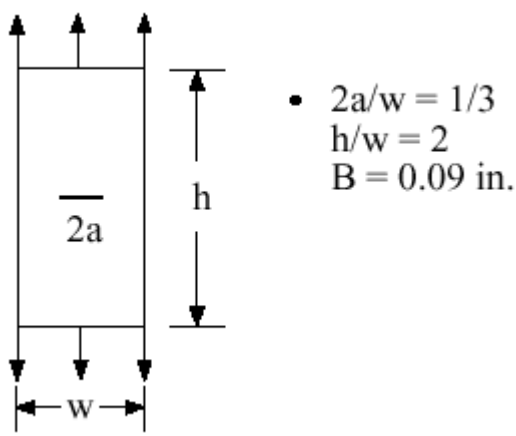


*Figure FAC-4.6. Test configuration for MT specimens.*

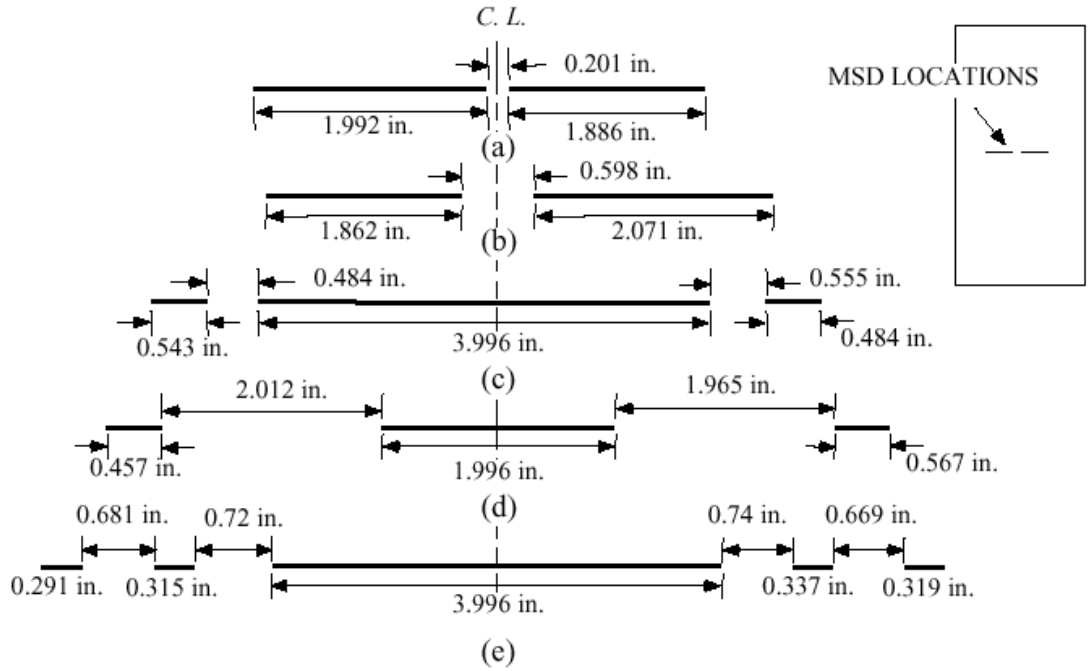


*Figure FAC-4.7. Schematic of crack configurations for12- inch MT specimens.*

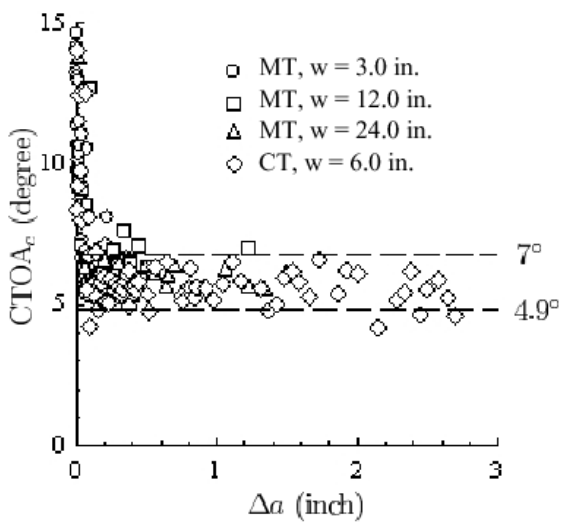


*Figure FAC-4.8. Surface measurements of CTOA$_c$ [from Dawicke1998]*

A special five-noded shell element, formulated by combining two four-noded elements and using linear constraint along the edge to eliminate the dependent node, is used to transition from locally refined zones around the crack path to a coarse mesh away from the crack.

A convergence study was conducted to determine the sensitivity of the predicted residual strength to the element size along the crack extension path. Three meshes for the 24-inch wide panel were created with crack tip element sizes of 0.04-inch, 0.02-inch, and 0.01-inch. For all crack growth and residual strength analyses, the CTOA is evaluated at 0.04-inch behind the crack tip to be consistent with experimental measurements. A finite element mesh with 0.04-inch square crack tip elements for the 24-inch wide panel is shown in Figure FAC-4.10. Predicted crack growth results for cases with 0.04-inch and 0.02-inch crack tip elements as well as predicted residual strengths for all three cases are shown in Figure FAC-4.11. Although some discrepancy is observed at the early stage of stable tearing, the predicted results exhibit little influence of mesh size after a relatively small amount of stable crack growth. More importantly, the predicted residual strength is very insensitive to crack tip element size. Thus, all the remaining meshes used in this example have 0.04 inch crack tip elements.

Figure FAC-4.12 shows two predicted crack opening profiles for the 24-inch wide panel. The angles are computed immediately after propagation (i.e., $CTOA_a$, see Figure FAC-4.2) with relaxation procedures completed and before increasing the applied displacement. The two $CTOA_a$ values correspond to (1) the angle after the first increment of crack growth, and (2) the angle after the specimen reaches its residual strength. As shown in the figure, $CTOA_a$ is much smaller than the critical angle after the first crack growth increment. This clearly demonstrates the permanent plastic deformation effects on stable crack growth in the elastic-plastic material. As the crack propagates, $CTOA_a$ increases. Since the analyses are conducted under displacement control, the $CTOA_a$ at residual strength is less than, but approaching its critical value.

Comparisons between numerical results and experimental measurements for the applied stress versus half crack extension are shown in Figure FAC-4.13. Results of predicted residual strength are comparable to experimental measurements, but as the width of the panel increases, the relative difference between experimental measurements and numerical predictions increases. Figure FAC-4.14 depicts the predicted plastic zone as the specimens reach their ultimate strength.

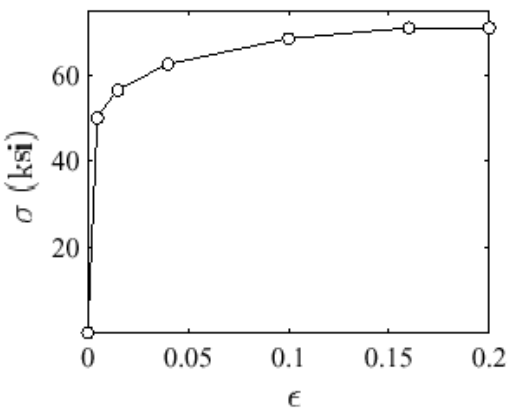


| σ (ksi) | ϵ |
|---|---|
| 0.0 | 0.0 |
| 50.0 | 0.00483 |
| 56.5 | 0.015 |
| 62.5 | 0.040 |
| 68.5 | 0.1 |
| 71.0 | 0.16 |
| 71.0 | 0.2 |

*E = 10350 ksi*
*ν = 0.3*

*Figure FAC-4.9. Piecewise linear representation of uniaxial stress-strain relationship for 2023-T3 aluminum alloy used in the present example.*

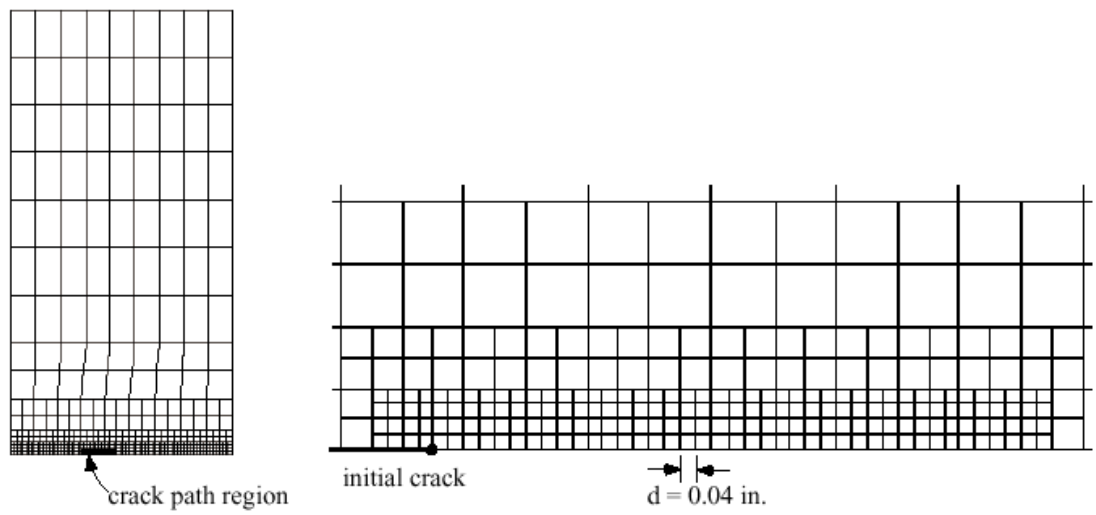


*Figure FAC-4.10. Finite element mesh for 24- inch wide MT specimen and detail along crack path.*

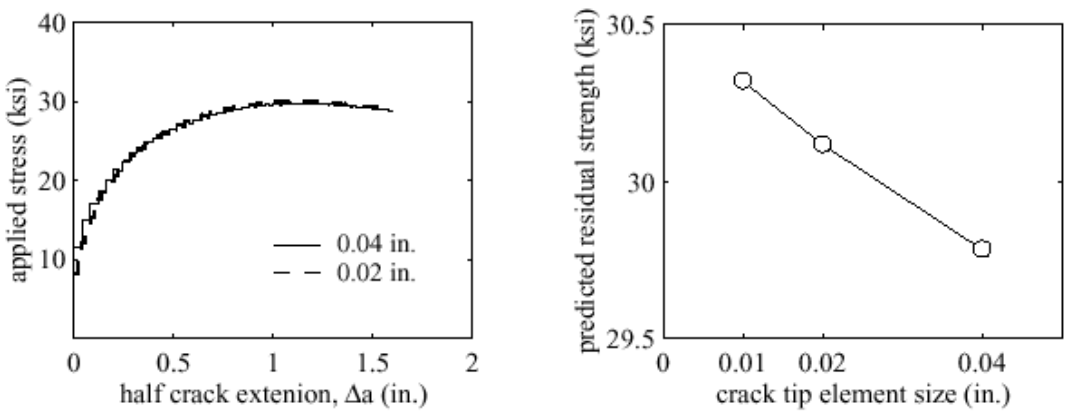


*Figure FAC-4.11. Results from convergence study: predicted crack growth and predicted residual strength for 24- inch wide panel with different crack tip element sizes.*

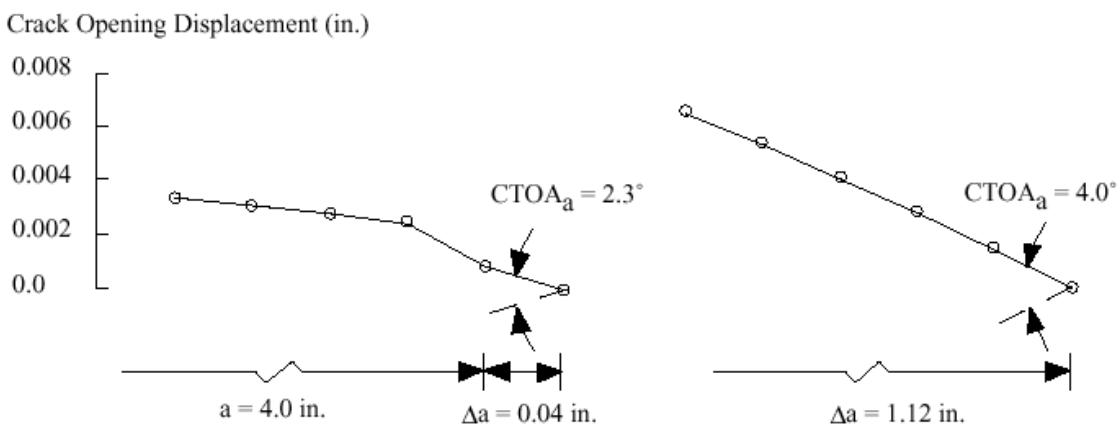


*Figure FAC-4.12. Crack opening profiles and CTOA a after the first crack growth increment and after reaching the residual strength for 24 inch wide panels.*

Two distinct phenomena are observed. For small specimens, plastic zones reach the free edge and the limit load is attained due to net section yielding. In contrast, for large specimens, plastic zones are well-confined by the elastic region and residual strength is reached near the fracture instability of the specimens.

As shown in Figure FAC-4.13, the relative difference in residual strength between experimental and numerical results increases as the width of the panel increases. This discrepancy is believed to be due to the three-dimensional nature of the stresses around the crack tip, a result of constraint effects due to the finite thickness of the panels [Hom 1990; Dawicke 1995]. Numerical results using plane strain, plane stress with a plane strain core height (see Figure FAC-4.5) equal to 0.12 inch, and three-dimensional finite

element analyses obtained from [Dawicke 1996, 1998] were studied to further demonstrate constraint effects on residual strength predictions. Predicted results shown in Table FAC-4.1 and Figure FAC-4.15 suggest that:

- Thin shell finite element analysis, behaving essentially in plane stress, tends to over-predict the residual strength as the width of the panel increases;
- Plane strain analysis over-predicts the residual strength of small specimens, but under-estimates it for large specimens;
- 2D plane stress analysis with a plane strain core and 3D analysis properly account for constraint effects. The predicted results follow the trend of experimental measurements even for wide panels.

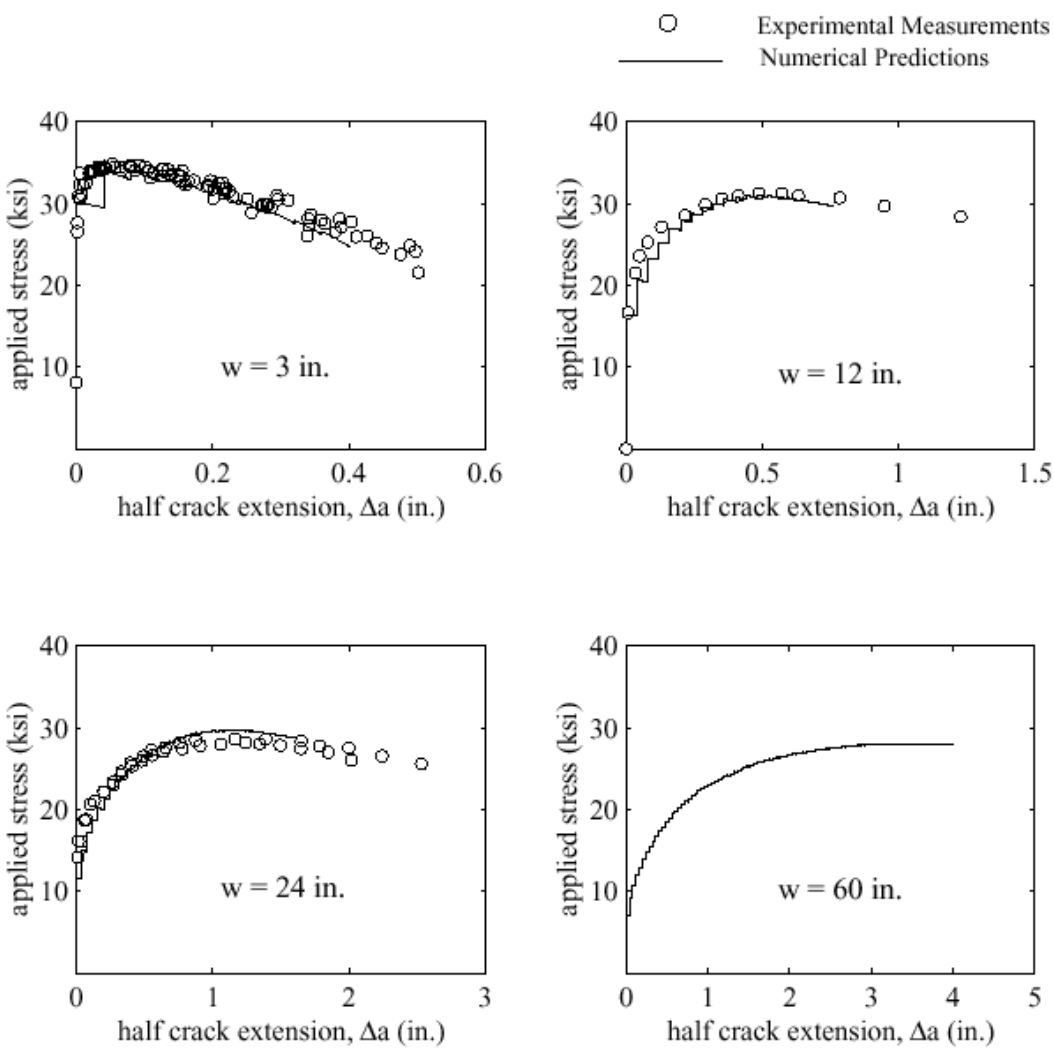


*Figure FAC-4.13. Comparisons between experimental measurements and numerical predictions of applied stress versus half crack extension for various sizes of specimens.*

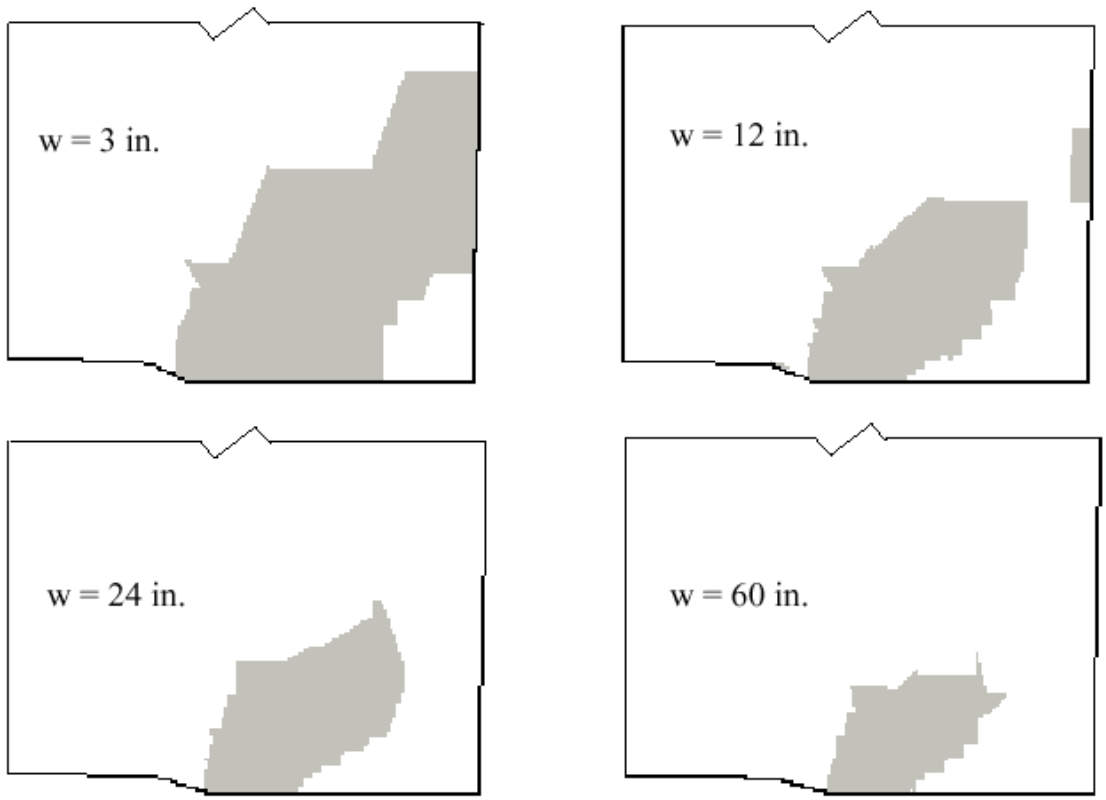


*Figure FAC-4.14. Numerical predictions of plastic zone for various sizes of specimens reaching their residual strength.*

*Table FAC-4.1 Comparisons of Residual Strength Predictions (ksi) for MT Specimens*

| Plate Width | Thin Shell | Plane Strain | Plane Strain Core | 3D | Experiment |
|---|---|---|---|---|---|
| 3 in. | 34.0 | 38 | 33.6 | 34.3 | 34.5 |
| 12 in. | 30.7 | 32.7 | 30.7 | 30.8 | 31.3 |
| 24 in. | 29.6 | 26.3 | 29.1 | 29.1 | 28.4 |
| 60 in. | 28.1 | 16.6 | 26.7 | 26.3 | N/A |

The cross-over between plane stress and plane strain in predicting residual strength as the specimen size increases is an interesting topic. Based on the predicted plasticity distribution in Figure FAC-4.14, the net section yielding mechanism seems to dominate the residual strength prediction of small specimens. This may explain why the plane strain analysis predicts a higher residual strength for small specimens because the effective yield stress in plane strain is larger than that in plane stress. Thus, a further increase of remote stresses under plane strain conditions is needed for specimens to reach the point of net section yielding. For larger specimens, residual strength is governed by

stable crack growth and fracture. As one would expect from the thickness effects on $K_c$ in LEFM, materials in plane stress have higher fracture toughness than materials in plane strain. Recent micromechanics-based, 3D analysis of ductile crack growth in a thin plate with a Gurson-type model also showed that, although the crack growth resistance at first increases with increasing plate thickness, the resistance to crack growth decreases after a small amount of crack extension [Mathur 1996]. For CTOA-driven ductile crack growth, stresses and strains under plane stress and plane strain conditions have not been studied in sufficient detail to clarify the issue. A possible cause of higher crack growth resistance in plane stress may be related to the residual plastic deformation effects. Based on asymptotic solutions for cracks growing in an incompressible elastic-perfectly plastic material under Mode I loading, larger residual plastic deformations would occur under plane stress than plane strain conditions leading to higher crack growth resistance.

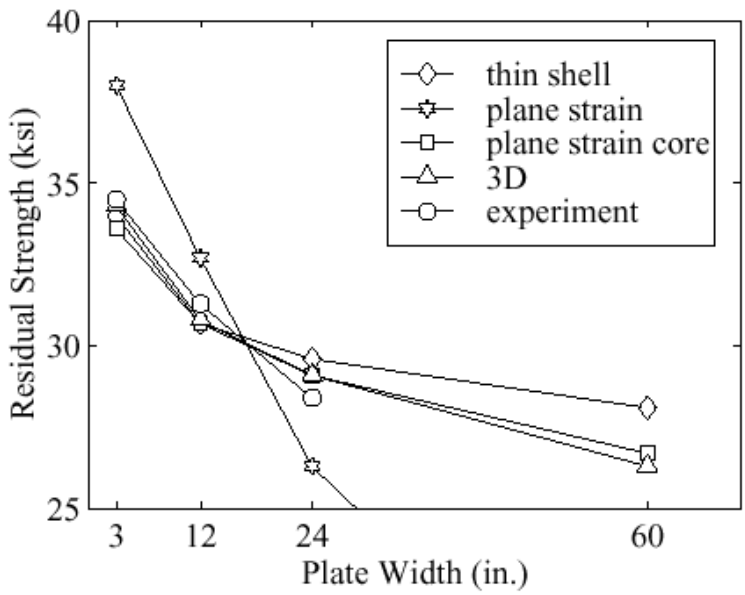


*Figure FAC-4.15. Predicted results of thin shell, plane strain, plane stress with a plane strain core, and 3D analyses compared with experimental measurements.*

*Numerical Simulations of Specimens with Multiple Cracks*

Numerical simulations of tests with multiple cracks using the CTOA fracture criterion are straightforward extensions of single crack specimen simulations. The same criterion ($CTOA_c$ = 5.25 degrees measured 0.04-inch behind the crack tip) is used to simulate stable crack growth and the link-up of multiple cracks, and to predict residual strength. No supplementary criterion is needed. Multiple crack test configurations as shown in Figure FAC-4.7 are modeled and the fracture processes are simulated. Note that the symmetry conditions along the vertical central line of the specimens are no longer valid due to the various lengths of fatigue pre-cracks; thus, at least one half of the specimen needs to be modeled. An example finite element mesh for test configuration b is shown in

Figure FAC-4.16. Mesh patterns around the multiple cracks are similar to those of the single crack models.

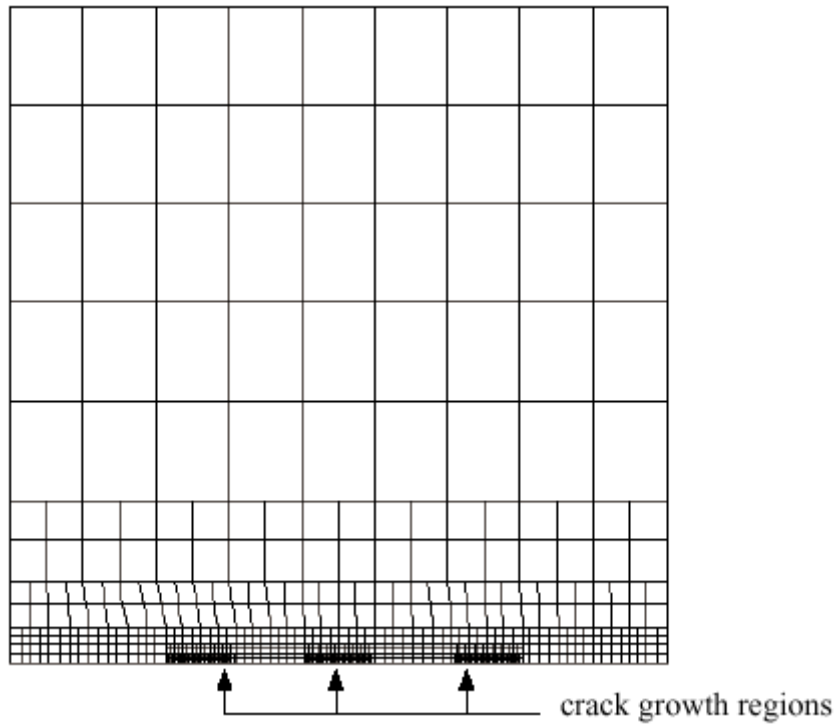


*Figure FAC-4.16. Finite element mesh for the test configuration b (12-inch wide specimen with two cracks).*

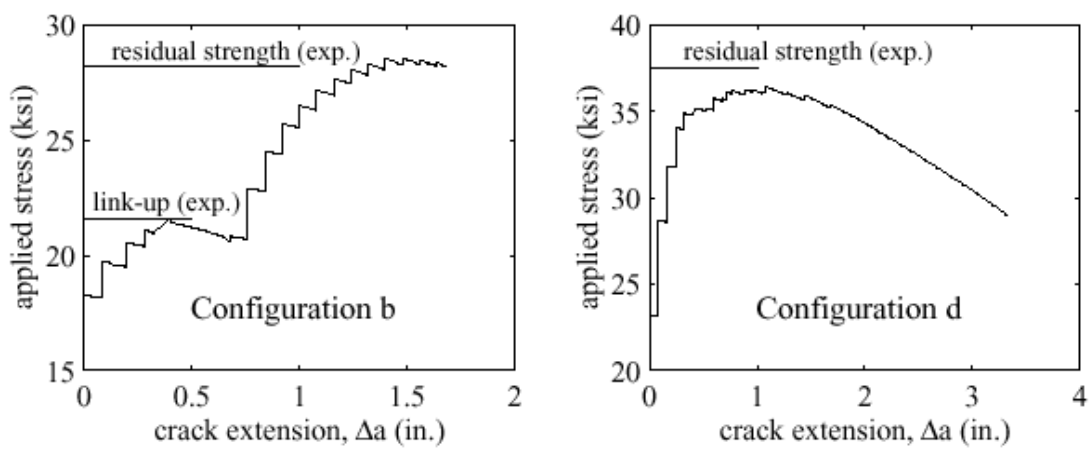


*Figure FAC-4.17. Predicted applied stress versus crack extension for test configurations b and d.*

Numerical results and experimental measurements for the applied stress versus half crack extension for test configuration b and d are shown in Figure FAC-4.17. Two distinct applied load versus crack growth history curves are predicted. For test configurations a, b, and c, link-up of cracks happens before the specimens reach their residual strength. For test configurations d and e, the limit load is attained before link-up. These numerical predictions agree with observations from the fracture tests. Again, plastic deformation plays an important role in the fracture process. Figure FAC-4.18 shows the plastic zone evolution of test configuration b during stable crack growth. The inherent residual plastic deformations during crack growth are clearly demonstrated through the deformed shapes.

Figure FAC-4.19 summarizes the relative difference between predicted results and experimental measurements. The predicted residual strength of all five MSD simulations agrees very well (within 3%) with experimental data. The predicted link-up load is comparable to experimental measurements, but the difference is larger than that for the residual strength. Reasons for the discrepancy may be related to the difficulty in measuring link-up load during the fracture tests. It is of practical importance to characterize the reduction in residual strength caused by MSD. Figure FAC-4.20 plots numerical predictions of residual strength versus lead crack length for cases with and without small cracks. A loss of residual strength due to the presence of multiple small cracks is observed.

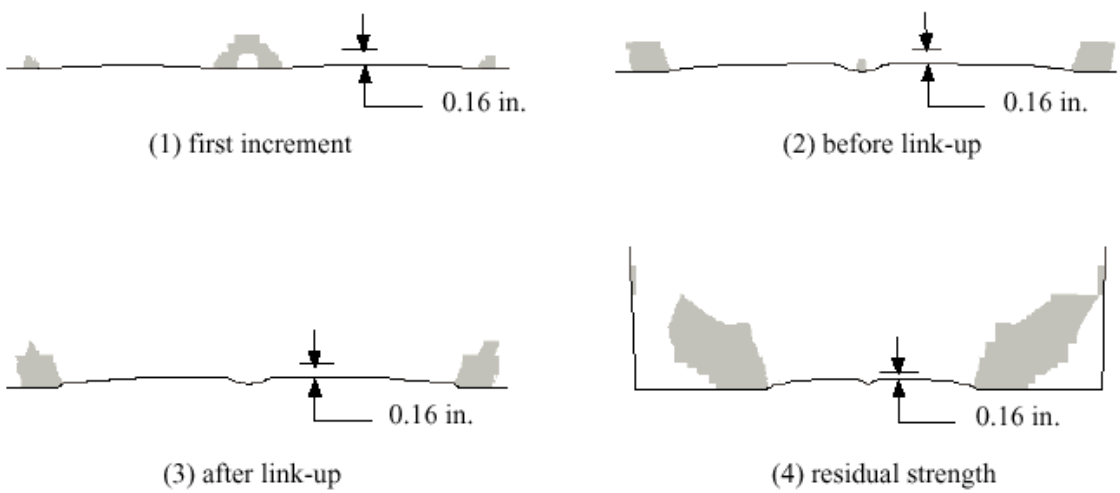


*Figure FAC-4.18. Crack opening profile(s) and plastic zone evolution of test configuration b during crack growth: (1) at the first increment, (2) before link-up, (3) after link-up, and (4) reaching residual strength.*

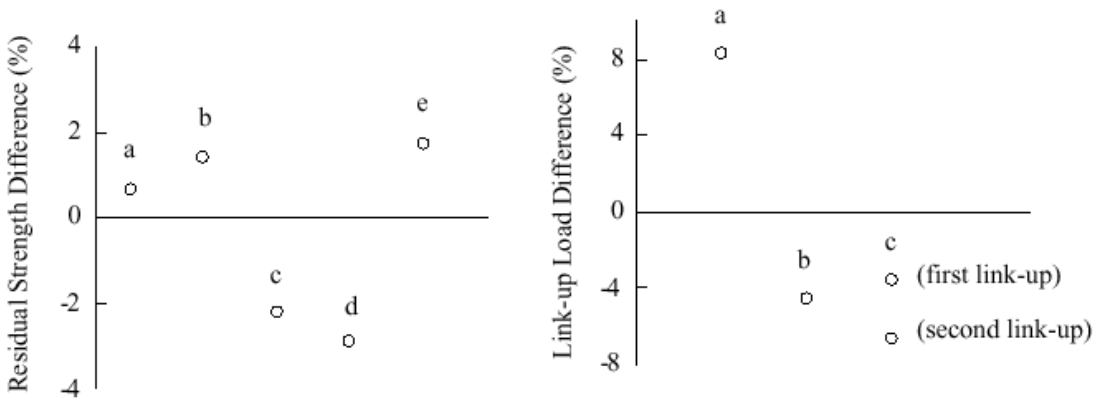


*Figure FAC-4.19. Relative difference of residual strength and link-up load between predicted results and experimental measurements for specimens with multiple cracks.*

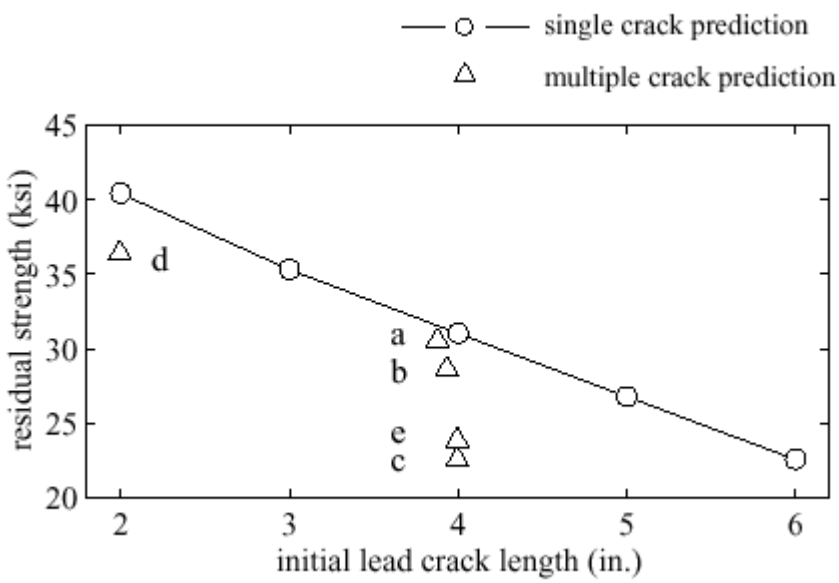


*Figure FAC-4.20. Loss of residual strength due to the presence of small cracks.*

## References

D. Broek, D. Y. Jeong, and T. P. Forte. Testing and Analysis of Flat and Curved Panels with Multiple Cracks. In *Proceedings of the FAA-NASA Sixth International Conference on the Continued Airworthiness of Aircraft Structures*, pp 85-98, Atlantic City, New Jersey, 1994.

C.-S. Chen, P. A. Wawrzynek, and A. R. Ingraffea. Simulation of Stable Tearing and Residual Strength Prediction with Applications to Aircraft Fuselages. In *Proceedings of*

*the FAA-NASA Symposium on Continued Airworthiness of Aircraft Structures*, pp 605-618, 1996.

C.-S. Chen, P. A. Wawrzynek, and A. R. Ingraffea. Recent Advances in Numerical Simulation of Stable Crack Growth and Residual Strength Prediction. In *Proceedings of the Sixth East Asia-Pacific Conference on Structural Engineering & Construction*, pp 1773-1778, 1997.

C.-S. Chen, P. A. Wawrzynek, and A. R. Ingraffea. Elastic-Plastic Crack Growth Simulation and Residual Strength Prediction of Thin Plates with Single and Multiple Cracks. In *Fatigue and Fracture Mechanics: 29th Volume, ASTM STP 1332*, 1998.

D. S. Dawicke, M. Sutton. CTOA and Crack-tunneling Measurements in Thin Sheet 2024-T3 Aluminum Alloy. *Experimental Mechanics*, Volume 34, pp 357-368,1994a.

D. S. Dawicke, J. C. Newman, Jr., M. A. Sutton, and B. E. Amstutz. Influence of Crack History on the Stable Tearing Behavior of a Thin-Sheet Material with Multiple Cracks. In *Proceedings of the FAA-NASA Sixth International Conference on the Continued Airworthiness of Aircraft Structures*, pp 193-212, Atlantic City, New Jersey, 1994b.

D. S. Dawicke, M. A. Sutton, J. C. Newman, Jr., and C. A. Bigelow. Measurement and Analysis of Critical CTOA for an Aluminum Alloy Sheet. In *Fracture Mechanics: 25th Volume, ASTM STP 1220,* Philadelphia, pp 358-379, 1995.

D. S. Dawicke. Residual Strength Predictions Using a Crack Tip Opening Angle Criterion. In *Proceedings of the FAA-NASA Symposium on the Continued Airworthiness of Aircraft Structures*, pp 555-566, Atlanta, Georgia, 1996.

D. S. Dawicke, R. S. Piascik, and J. C. Newman, Jr. Prediction of Stable Tearing and Fracture of a 2000-Series Aluminum Alloy Plate Using a CTOA Criterion. In *Fracture Mechanics: 27th Volume, ASTM STP 1296*, Philadelphia, pp 90-104, 1997a.

D. S. Dawicke and J. C. Newman, Jr. Evaluation of Various Fracture Parameters for Predictions of Residual Strength in Sheets with Multi-Site Damage. In *Proceedings of the First Joint DoD/FAA/NASA Conference on Aging Aircraft*, Ogden, Utah, July 1997b.

D. S. Dawicke and J. C. Newman, Jr. Residual Strength Predictions for Multiple Site Damage Cracking Using a Three-Dimensional Analysis and a CTOA Criterion. In **F***atigue and Fracture Mechanics: 29th Volume, ASTM STP 1332*, 1998.

A. U. de Koning. A Contribution to the Analysis of Quasi-Static Crack Growth in Steel Materials. In *Fracture 1977, Proceedings of the 4th International Conference on Fracture*, Volume 3, pp 25-31, 1977.

C. L. Hom and R. M. McMeeking. Large Crack Tip Opening in Thin Elastic-Plastic Sheets. *International Journal of Fracture*, Volume 45, pp 103-122, 1990.

M. F. Kanninen and C. H. Popelar. *Advanced Fracture Mechanics*. Oxford University Press, New York, 1985.

K. K. Mathur, A. Needleman, and V. Tvergaard. Three Dimensional Analysis of Dynamic Ductile Crack Growth in a Thin Plate. *Journal of the Mechanics and Physics of Solids*, Volume 44, pp 439-464, 1996.

J. C. Newman, Jr. Finite-Element Analysis of Fatigue Crack Propagation-Including the Effects of Crack Closure. Ph.D. Thesis, Virginia Polytechnic Institute, 1974.

J. C. Newman, Jr. An Elastic-Plastic Finite Element Analysis of Crack Initiation, Stable Crack Growth, and Instability. In *Fracture Mechanics: Fifteenth Symposium, ASTM STP 833*, Philadelphia, pp93-117, 1984.

J. C. Newman, Jr. An Evaluation of Fracture Analysis Methods. In *Elastic-Plastic Fracture Mechanics Technology, ASTM STP 89***6**, Philadelphia, pp5-96, 1985.

J. C. Newman, Jr., D. S. Dawicke, and C. A. Bigelow. Finite-Element Analysis and Fracture Simulation in Thin-Sheet Aluminum Alloy. In *Proceedings of the International Workshop on Structural Integrity of Aging Airplanes*, 1992.

J. C. Newman, Jr., D. S. Dawicke, M. A. Sutton, and C. A. Bigelow. A Fracture Criterion For Widespread Cracking in Thin-Sheet Aluminum Alloys. In *International Committee on Aeronautical Fatigue, 17th Symposium*, Stockholm, Sweden, 1993.

C. C. Rankin and F. A. Brogan. The Computational Structural Mechanics Testbed Structural Element Processor ES5: STAGS Shell Element, 1991. NASA CR-4358.

J. R. Rice. Elastic-Plastic Models for Stable Crack Growth. In *Mechanics and Mechanisms of Crack Growth*, May, M. J. ed., British Steel Corp. Physical Metallurgy Center Publication, Sheffield, England, pp14-39, 1975.

J. R. Rice and E. P. Sorensen. Continuing Crack-Tip Deformation and Fracture for Plane-Strain Crack Growth in Elastic-Plastic Solids. *Journal of the Mechanics and Physics of Solids*, Volume 26, pp163-186, 1978.